RSC Advances

ROYAL SOCIETY OF CHEMISTRY

www.rsc.org/advances

JournalName

RSCPublishing

COMMUNICATION

$NaTi_3FeO_8$: a novel anode material for sodium-ion batteries

Cite this: DOI: 10.1039/x0xx00000x

Junke Hou[a,b], Yubin Niu[a,b], Fenglian Yi[a,b], Sangui Liu[a,b], Yutao Li[c], Hong He[a] and Maowen Xu[a,b*]

Received 00th January 2012,
Accepted 00th January 2012

DOI: 10.1039/x0xx00000x

www.rsc.org/

A novel $NaTi_3FeO_8$ material is explored as an anode for sodium-ion batteries for the first time. It delivers a reversible discharge capacity of 170.7 mA h g^{-1} at 20 mA g^{-1} in a sodium half cell, exhibiting good capacity retention at a cut-off voltage of 0.01 ~ 3 V.

In recent years, electric vehicles or smart grid systems have become a new frontier of rechargeable batteries together with the global environmental issues. In such a large scale system, both cost and cycle performance of the rechargeable batteries are as important as fundamental characteristics, which leads to a rediscovery of sodium-ion batteries with low cost electrodes.[1–2]

Suitable electrode materials with high reversible capacity and long-term stability play a significant role in realizing the large-scale energy storage. Although a variety of materials with good features in terms of capacity and voltage can be used potentially as positive electrodes[3], hard carbonaceous materials can insert and de-insert sodium ions during a charge and discharge cycle, but they exhibit larger capacity fade than their lithium counterparts.[4] many materials[5-10] have been reported to be useful as negative electrodes in sodium-ion batteries, however, they still exist some problems, such as the cycle life is poor,[8] the preparation method is complex,[10] and so on. Therefore the sodium ion battery utility is quite a distance.

More recently, $Na_xM_yO_z$ (M = Ti, Fe, Co and Ni) anode materials with layered structure have been studied for sodium-ion batteries (such as $Na_{2.65}Ti_{3.35}Fe_{0.65}O_9$ can obtain a reversible capacity of 137.5mA h g^{-1} at a current rate of 40 mA g^{-1}), and they have begun to attract increasing attention for their unique advantages, such as simple synthesis, low cost and long cycle life.[11-15] $Na_xTi_yO_z$ anode materials with good electrochemical performance have been studied for sodium-ion batteries.[15-17] $NaTi_3FeO_8$[18-19] with one dimensional sodium ion transport channel , could be very promising anode materials for sodium batteries. Here we used a simple method to synthesize $NaTi_3FeO_8$, and tested its performance in sodium ion battery for the first time. As an anode material for sodium-ion battery, although the measured capacity relative to the theoretical capacity (229 mA h g^{-1}) is not high, it has a low voltage plateau and long cycle life.

$NaTi_3FeO_8$ samples were synthesized by solid-state reaction of stoichiometric amounts of Na_2CO_3, Fe_2O_3 and TiO_2. The powders were ball-milled with ethanol for 10 h at 500 rpm, and dried for 12 h at 100 °C. Finally, the obtained powders were heated at 950 °C for 12 h in an Air atmosphere. The anode electrodes were prepared by mixing active material, super-P carbon black, and polyvinylidene fluoride (PVdF) in a weight ratio 80: 10: 10 with Nmethyl pyrrolidone (NMP) as solvent. The anode electrodes were pressed onto the copper foil and dried at 120 °C under vacuum for 12 h. The CR2032 coin-type cells consisting of a cathode and sodium metal anode separated by a glass fiber were assembled in a glove box filled with dry argon gas. The electrolyte was 1 M $NaPF_6$ in ethylene carbonate–diethyl carbonate (EC/DEC, 1:1 (v/v)) (Sigma). The geometrical area of the electrode was 1.0 cm^2. The active material in the electrode was around 1.5 mg. The galvanostatic charge–discharge tests were performed using a Land battery tester at different rates at 25 °C after 12 h rest.

Powders X-ray diffraction were performed using Cu Kα radiation on a Bruker D8 Advance Diffractometer (XRD,

Maxima-X XRD-7000), X-ray photoelectron spectroscopy (XPS) measurements were carried out on a spectrometer (Escalab 250xi, Thermo Scientific) and the morphology of as-prepared materials were also observed using field-emission scanning electron microscopy (FESEM, JSM-6700F).

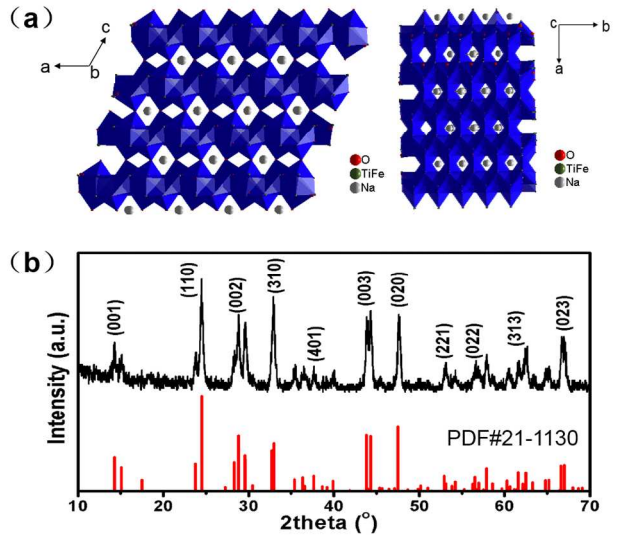

Figure 1 (a) Schematic illustration of the crystal structure of $NaTi_3FeO_8$; (b) XRD pattern of the as-prepared $NaTi_3FeO_8$ sample.

Fig. 1(a) schematically shows that the framework of $NaTi_3FeO_8$ is built of $(Fe/Ti)O_6$ octahedral with sharing edges, and the larger sodium ions occupy the distorted octahedral sites with four short Na-O bonds. The Na^+ can transfer along the b-axis and c-axis direction, especially along the b-axis with much shorter Na^+-Na^+ distance. The XRD pattern of the sample is shown in Fig. 1(b), although some characteristic diffraction peaks of the as-obtained sample can match well with the standard XRD pattern of $NaTi_3FeO_8$ (PDF#21-1130), there are still other diffraction peaks near 20º arising from the possible impurity phases such as Fe_2O_3.

Structural details and composition of $NaTi_3FeO_8$ were obtained with XPS analysis. The XPS spectra of $NaTi_3FeO_8$ is displayed in Fig. 2. The wide angle XPS (Fig. 2a) of the obtained samples shows the predominant presence of O, Ti, Fe, and Na. The position of peaks are 710.9 eV ($Fe3^+$, $Fe2p_{3/2}$), 458.5 eV (Ti^{4+}, $Ti2p_{3/2}$), 457.8 (Ti^{4+}, $Ti2p_{3/2}$), 530.5 eV (O^{2-}, O1s), 530.5 eV (O^{2-}, O1s) and 529.3 eV (O^{2-}, O1s) (Fig. 2b-d), respectively. The valence of the Fe, O, Ti is +3, -2 and +4, respectively, which is consistent with the XPS results.[20] The atomic percentages of samples are 2.81%, 8.43%, 2.85%, and 22.88% for Na, Ti, Fe, and O.

The FESEM images of as-prepared $NaTi_3FeO_8$ samples are shown in Fig. 3(a) and Fig. 3(b). A higher magnification image reveals that the length of rod-shaped $NaTi_3FeO_8$ is not uniform and the width is 200 ~ 500 nm. As shown in Fig. 3(c-f), the energy-dispersive X-ray (EDX) mappings show no impurities, and all four elements – Na, Ti, Fe and O are present uniformly throughout the bulk of the sample, which is consistent of XPS. Fig.S1 shows the SEM images of $NaTi_3FO_8$ after 200 cycles. From the figure we can see the morphology of the material is substantially unchanged.

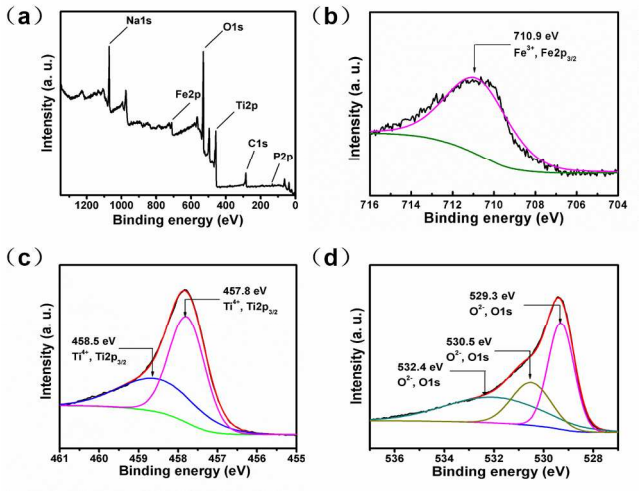

Figure 2 XPS survey spectrum of $NaTi_3FeO_8$.

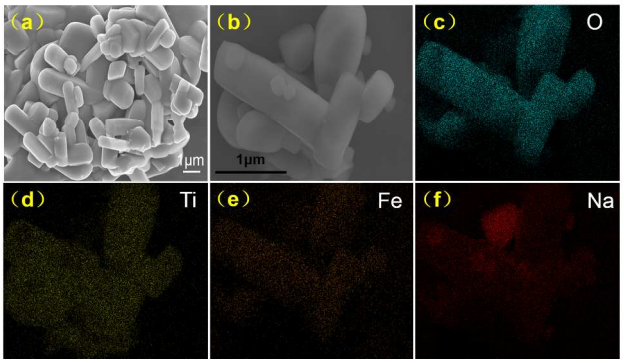

Figure 3 (a) and (b) SEM images of the $NaTi_3FeO_8$ with different magnifications; (c), (d), (e) and (f) EDX-element distribution mapping images of $NaTi_3FeO_8$.

The sodium insertion–extraction behavior of $NaTi_3FeO_8$ is studied by galvanostatic charge–discharge test as shown in Fig. 4. The differential specific capacity plots of the 1st, 2nd and 3rd cycle are shown in Fig. 4(a). The first charge–discharge capacity is 148.9/327.4 mA h g^{-1} at a current rate of 20 mA g^{-1}, respectively. The following charge–discharge capacities are 147.5/170.7 mA h g^{-1} and 147.1/162.5 mA h g^{-1} in the 2nd and 3rd cycle, respectively. Fig.S2 shows that when the cell was discharged to 0.01V, the position of peaks are 458.2 eV (Ti^{4+}, $Ti2p_{3/2}$), 459.2 eV (Ti^{4+}, $Ti2p_{3/2}$), 464.8 eV (Ti^{4+}, $Ti2p_{3/2}$) and 462.3 eV (Ti^{3+}, $Ti2p_{1/2}$), the valences of Ti are +3 and +4. This suggests that the following reaction taken place in the charge/discharege process: Ti^{4+} + e^- ↔ Ti^{3+}. The electrochemical equation for sodium storage can hence be stated as follows: $1/3NaTi_3FeO_8 + xNa^+ + xe^-$

$\leftrightarrow$ $1/3Na_{1+x}Ti_3FeO_8$ with x = 0.745 (x = 1 refers to the theoretical capacity of 229 mA h g^{-1} corresponding to 3 mole of charge storage).[21]

To understand the electrochemical sodium-ion insertion-extraction processes clearly in the first three cycles, cyclic voltammetry studies were performed on $NaTi_3FeO_8$. As shown in Fig. 4 (b), it can be seen that the first cycle reduction process consists of two peaks (at 0.01 V and 0.61 V). On the subsequent cycling, the 0.61 V reduction peak shifts to 0.55 V. The first cycle oxidation process has two peaks at 0.35 V and 0.74 V. The 0.35 V oxidation peak vanishes completely while the 0.74 V oxidation peak intensifies and shifts to 0.79 V on the subsequent cycling. The irreversible peaks were observed, which were caused by the solid electrolyte interface (SEI) layer formation, irreversible sites for sodium-ion insertion in the crystal lattice defects, electrolyte, and other organic material decomposition.[22-23]

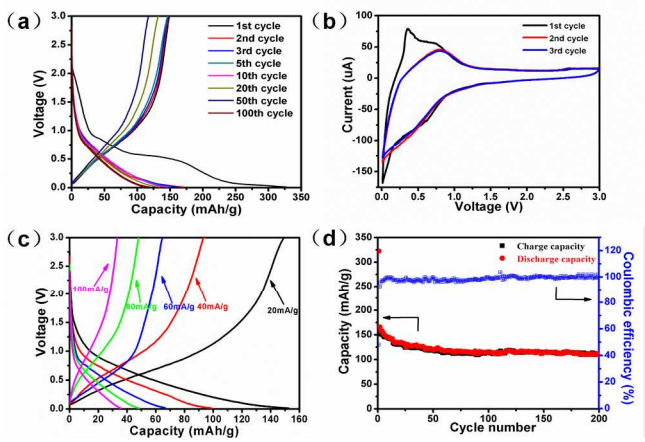

Figure 4 Performance of $NaTi_3FeO_8$. (a) The 1st, 2nd and 3rd discharge/charge curves of $NaTi_3FeO_8$ at a current rate of 20 mA g^{-1} in the voltage range of 0.01 and 3 V versus Na^+/Na; (b) Cyclic voltammogram curves at a scan rate of 0.1 mV s^{-1} showing the first, the second and the third cycle of the $NaTi_3FeO_8$ composite electrode at a voltage window of 0.01 ~ 3 V; (c) Long-term cycling performance of the $NaTi_3FeO_8$ at a current rate of 20 mA g^{-1} in the voltage range of 0.01 and 3 V versus Na^+/Na; (d) Rate capability of the $NaTi_3FeO_8$. The capacity versus cycle number at various current rates.

The rate performance of the $NaTi_3FeO_8$ composite electrode is summarized in Fig. 4 (c). The cell was cycled at five different rates of 20, 40, 60, 80 and 100 mA g^{-1} in a voltage window of 0.01 ~ 3 V. The cell delivers large reversible capacity of 98.9 mA h g^{-1} (64.8% of that at 20 mA g^{-1}) with small polarization even at a discharge rate of 40 mA g^{-1}, while the discharge capacity of the $NaTi_3FeO_8$ electrode material can still deliver 35.8 mA h g^{-1} at a rate of 100 mA g^{-1}. The cycling stability and the coulombic efficiency are also displayed in Fig. 4 (d), and the capacity is still maintained at 110.5 mA h g^{-1} at a current rate of 20 mA g^{-1} after 200 cycles, and the corresponding capacity retention is 66.7%, and the coulombic efficiency is close to 100% except the first cycle, showing good cycling stability. Although the rate capacity of the $NaTi_3FeO_8$ as a new anode material is not as high as hard carbon[4], its cycling stability is much better. The poor rate performance could be due to its low electric conductivity. In the next step, we will improve its electric conductivity by coating or doping, thereby enhancing the capacity and rate performance. The good cycle life of $NaTi_3FeO_8$ cells are mostly attributed to the structure stability of the $NaTi_3FeO_8$ electrode material during sodium-ion insertion–extraction processes.[24-25] Therefore, the $NaTi_3FeO_8$ electrode material is promising in practical sodium-ion batteries because of its good reversible structure change after sodium ion extraction–insertion processes.

In summary, we have synthesized $NaTi_3FeO_8$ by a simple solid-state route. The as-obtained sample is of mainly micrometer sizes. The sodium-ion extraction–insertion behavior of $NaTi_3FeO_8$ is investigated in detail for the first time. It delivered a discharge capacity of 170.7 mA h g^{-1} at a current density of 20 mA g^{-1}, and it presents a good capacity retention.

Acknowledgements

This work is financially supported by Chongqing Key Laboratory for Advanced Materials and Technologies of Clean Energies under cstc2011pt-sy90001, Start-up grant under SWU111071 from Southwest University and Chongqing Science and Technology Commission under cstc2012gjhz90002. The work is supported by grants from Fundamental Research Funds for the Central Universities (SWU113079, XDJK2014C051) and Research Funds for a Postdoctor of Chongqing (XM2014097).

Notes and references

[a]*Institute for Clean Energy & Advanced Materials, Faculty of Materials and Energy， Southwest University, Chongqing 400715, P.R. China*
[b]*Chongqing Key Laboratory for Advanced Materials and Technologies of Clean Energies, Chongqing 400715, P.R. China*
[c]*Texas Materials Institute, University of Texas at Austin, Texas 78712, USA*
Fax: +86-23-68254969; Tel: +86-23-68254969;
E-mail: xumaowen@swu.edu.cn

1 Y. Kawabe, N. Yabuuchi, M. Kajiyama, N. Fukuhara, T. Inamasu, R. Okuyama, I. Nakai, S. Komaba, *Electrochem. Commun.*, 2011, **13**, 1225.
2 K. Trad, D. Carlier, L. Croguennec, A. Wattiaux, M. Ben Amara, C. Delmas, *Chem. Mater.*, 2010, ***22,*** 5554.
3 R. Berthelot, D. Carlier, C. Delmas, *Nat. Mater.*, 2011, **10(1)**, 74.
4 R. Alcantara, J. M. JimenezMateos, J. L. Tirado, *J. Electrochem. Soc.*, 2002, **149**, A201.
5 L. Baggetto, J. K. Keum, J. F. Browning, G. M. Veith, *Electrochem. Commun.*. 2013, **34**, 41.
6 A. Kohandehghan, K. Cui, M. Kupsta, J. Ding, E. M. Lotfabad, W. P. Kalisvaart and D. Mitlin, *Nano Lett.*, 2014, **14**, 5872.
7 P. R. Abel, M. G. Fields, A. Heller and C. B. Mullins, *ACS Appl. Mater. Interfaces*, 2014, **6**, 15860.
8 B. Farbod, K. Cui, W. P. Kalisvaart, M. Kupsta, B. Zahiri, A. Kohandehghan, E. M. Lotfabad, Z. Li, E. J. Luber and D. Mitlin, *ACS Nano*, 2014, **8**, 4415.

9 C. Yue, Y. Yu, S. Sun, X. He, B. Chen, W. Lin, B. Xu, M. Zheng, S. Wu, J. Li, J. Kang and L. Lin, *Adv. Funct. Mater.*, 2015, **25**, 1386.
10 P. R. Abel, Y.-M. Lin, T. D. Souza, C.-Y. Chou, A. Gupta, J. B. Goodenough, G. S. Hwang. A. Heller and C. B. Mullins, *J. Phys. Chem. C*, 2013, **117**, 18885.
11 M. Sathiya, K. Hemalatha, K. Ramesha, J. M. Tarascon and A. S. Prakash, *Chem. Mater.*, 2012, **24**, 1846.
12 S. Komaba, W. Murata, T. Ishikawa, N. Yabuuchi, T. Ozeki, T. Nakayama, A. Ogata, K. Gotoh, K. Fujiwara. *Adv. Funct. Mater.*, 2011, **21**, 3859.
13 L. Xin, Y. Liu, B. Li, X. Zhou, H. Shen, W. Zhao and C. Liang, *Sci. Rep.*, 2014, **4**, 4479.
14 M. M. Doeff, J. Cabana and M. Shirpour, *J. Inorg Organomet Polym*, 2014, **24**, 5.
15 M. Xu, J.-K. Hou, Y.-B. Niu, G.-N. Li, Y.-T. Li and C. M. Li, *Chem. Commun.*, 2015, **51**, 3227.
16 Y. Wang, X. Yu, S. Xu, J. Bai, R. Xiao, Y. S. Hu, H. Li, X. Q. Yang, L. Chen and X. Huang. *Nat. Commun.*, 2013, **4**, 2365.
17 A. Rudola, K. Saravanan, C. W. Mason and P. Balaya. *J. Mater. Chem. A*, 2013, **1**, 2653.
18 M. N. Akieh, M. Lahtinen, A. Väisänen, M. Sillanpää, *J. Hazard. Mater.*, 2008, **152(2)**, 640.
19 J. Črnko, *Metalurgija*, 2002, **41(2)**, 67.
20 G. K. Mor, H. E. Prakasam, O. K. Varghese, K. Shankar and C. A. Grimes, *Nano Lett.*, 2007, ***7* (8)**, 2356.
21 A. Rudola, K. Saravanan, S. Devaraj, H. Gong and P. Balaya, *Chem. Commun.*, 2013, **49**, 7451.
22 S. Komaba, T. Ishikawa, N. Yabuuchi, W. Murata, A. Ito and Y. Ohsawa, *ACS Appl. Mater. Interfaces*, 2011, **3**, 4165.
23 K.-T. Kim, G. Ali, K. Y. Chung, C. S. Yoon, H. Yashiro, Y.-K. Sun, J. Lu, K.l Amine and S.-T. Myung, *Nano Lett.,* 2014, **14**, 416.
24 H. Kim, D. J. Kim, D.-H. Seo, M. S. Yeom, K. Kang, D. K. Kim and Y. Jung, *Chem. Mater.*, 2012, **24**, 1205.
25 E. Hosono, T. Saito, J. Hoshino, M. Okubo, Y. Saito, D. Nishio-Hamane, T. Kudo and H. Zhou, *J. Power Sources*, 2012, **217**, 43.